Electric and magnetic resonances in strongly anisotropic particles

Satoshi Ishii,* Shin-ichiro Inoue, and Akira Otomo

Advanced ICT Research Institute, National Institute of Information and Communications Technology, Kobe, Hyogo 651-2492, Japan
**Corresponding author: s.ishii@nict.go.jp*

Received November 1, 2013; revised December 4, 2013; accepted December 4, 2013; posted December 5, 2013 (Doc. ID 200602); published January 7, 2014

We show that a sphere made of a uniaxial medium with hyperbolic dispersion can exhibit both magnetic and electric resonances. The anisotropy conditions for the magnetic and electric resonances in a hyperbolic sphere are derived and verified by numerical simulation. The occurrence of both magnetic and electric resonances in a hyperbolic sphere indicates avenues for further study of metamaterial applications and scattering effects. © 2014 Optical Society of America

OCIS codes: (290.5850) Scattering, particles; (160.3918) Metamaterials; (160.1190) Anisotropic optical materials.
http://dx.doi.org/10.1364/JOSAB.31.000218

1. INTRODUCTION

In optics, particles are the simplest resonators in which resonance can be easily induced by any kind of light source. Metallic particles have attracted considerable attention due to their plasmonic resonance [1–3], and particles made of materials with a high refractive index (high-n materials) have also been studied extensively. A major reason for the strong interest in high-n particles is that they exhibit magnetic resonance that is the lowest-order resonance of an isotropic high-n particle: the first Mie resonance [4]. In contrast with metallic metamaterials, which require complex subwavelength structures and are lossy [5–7], high-n particles do not require complex structures to exhibit magnetic resonance, and low-loss resonance can be achieved. Magnetic resonance of high-n particles has been experimentally observed at gigahertz frequencies for ceramic rods [8] and cubes [9], in the mid-infrared range for silicon carbide rods [10] and tellurium cubes [11], and recently in the visible range for silicon spheres [12]. By arranging high-n particles in a periodic array, it is possible to obtain effectively negative permeability [8–11,13]. The next lowest resonance of isotropic high-n particles is electric resonance. In a same manner, electric resonance of high-n particles can be used to obtain effectively negative permittivity.

Furthermore, the occurrence of magnetic and electric resonances in a single high-n particle leads to exotic scattering patterns. First theoretically predicted by Kerker *et al.* [14], forward and backward scattering can be drastically suppressed even for nonmagnetic particles [15–17]. Under such suppressed forward and backward scattering conditions, the optical forces acting on a high-n particle are different even though the scattering cross sections are identical [18].

In addition to isotropic high-n particles, particles made of strongly anisotropic materials with hyperbolic dispersion can also exhibit both magnetic and electric resonances [19]. Because the effective refractive index inside a hyperbolic material is much greater than unity, a hyperbolic particle can be of subwavelength size even in the optical range. Hyperbolic materials have uniaxial anisotropy, where the principal components have opposite signs. Various crystals, such bismuth and sapphire [20], are hyperbolic in the far-infrared region. Additionally, it is possible to design effectively hyperbolic materials using metamaterials [21–23]. The mode volumes [24,25] and scattering properties [26] of hyperbolic particles have been analyzed, and electric and magnetic resonances have been observed even in initial experiments on particle arrays of hyperbolic metamaterials [19,25,27,28]. However, to date, the necessary conditions for hyperbolic particles to resonate have not been investigated. In this work, to stimulate research on hyperbolic particles, we provide a simple guideline for estimating the magnetic and electric resonances of hyperbolic spheres. Although spheres are chosen in order to compare the results with those of the Mie theory, the present results also hold for hyperbolic cubes and can be easily modified for application to hyperbolic cuboids. Our analysis should facilitate the process of finding particular resonance modes of hyperbolic particles for applications including, but not limited to, negative permeability and anisotropic scattering.

2. RESONANCE MODE ANALYSIS

The dispersion relation for monochromatic waves in a uniaxial material whose diagonal permittivity is $\varepsilon = \mathrm{diag}(\varepsilon_x, \varepsilon_x, \varepsilon_z)$ is expressed as [29]

$$\left(\frac{k_x^2+k_y^2}{\varepsilon_z}+\frac{k_z^2}{\varepsilon_x}-\frac{\omega^2}{c^2}\right)\left(\frac{k_x^2+k_y^2+k_z^2}{\varepsilon_x}-\frac{\omega^2}{c^2}\right)=0, \qquad (1)$$

where k_x, k_y, and k_z, are the x, y, and z components of the wave vector, respectively; ω is the angular frequency; and c is the speed of light. Equation (1) can be separated into two parts:

$$\frac{k_x^2+k_y^2}{\varepsilon_z}+\frac{k_z^2}{\varepsilon_x}=\frac{\omega^2}{c^2}, \tag{2}$$

$$\frac{k_x^2+k_y^2+k_z^2}{\varepsilon_x}=\frac{\omega^2}{c^2}. \tag{3}$$

Equations (2) and (3) are associated with extraordinary and ordinary waves, respectively. Only extraordinary waves produce hyperbolic dispersion, and ordinary waves produce circular dispersion.

In this work, we limit ourselves to considering a hyperbolic sphere in free space. Because of the large refractive index contrast between a hyperbolic sphere and free space, the boundary can confine the resonance modes. As we deal with only low-order resonance modes, we approximate the sphere as a cube with a side equal to the diameter of the sphere. Because of this approximation, our approach might deviate from the actual resonance in some cases. Nonetheless, it serves as a quick guideline for estimating the resonance as we present in the next section. At resonance, a lossless cavity satisfies the conditions

$$k_x=\frac{\pi l}{2r},\qquad k_y=\frac{\pi m}{2r},\qquad k_z=\frac{\pi n}{2r}, \tag{4}$$

where r is the radius of the sphere, and l, m, and n are nonnegative integers. By substituting Eq. (4) into Eqs. (2) and (3), we obtain

$$\frac{l^2+m^2}{\varepsilon_z}+\frac{n^2}{\varepsilon_x}=\frac{\omega_{lmn}^2}{\alpha}, \tag{5}$$

$$\frac{l^2+m^2+n^2}{\varepsilon_x}=\frac{\omega_{lmn}^2}{\alpha}. \tag{6}$$

Here, $1/\alpha=4r^2/(\pi^2c^2)$. For a hyperbolic sphere to resonate, the left side of either Eq. (5) or Eq. (6) must be positive. It is important to bear in mind that, for a hyperbolic sphere, the resonance frequencies for the modes associated with Eq. (5) are always higher than those for the modes associated with Eq. (6).

Next, we consider the conditions for the lowest-order mode (1, 1, 1) and the second-lowest order modes (1, 1, 2) and (2, 1, 1) for extraordinary waves, which have one antinode and two antinodes, respectively, in a magnetic field. As presented below, the electric displacement vectors of the lowest-order mode (1, 1, 1) form a loop, thus creating magnetic dipole resonance. One of the second-lowest modes, either (1, 1, 2) or (2, 1, 1), creates two electric displacement loops circulating in opposite directions to each other, thus giving rise to electric resonance. Modes (1, 1, 1) and (1, 1, 2) are similar to magnetic and electric resonance modes in high-n particles [9,11,12], respectively, which are explained by the Mie theory [4].

For the lowest-order mode (1, 1, 1) to be supported, the left side of Eq. (5) must be positive. The same holds for modes (1, 1, 2) and (2, 1, 1). Additionally, the mode (l,m,n) has to satisfy $l^2/\varepsilon_z+n^2/\varepsilon_x>0$ and $m^2/\varepsilon_z+n^2/\varepsilon_x>0$ at x–z and y–z cross sections, respectively. Below, we use the notation $\varepsilon'=\mathrm{Re}(\varepsilon)$. Table 1 summarizes the conditions for the three lowest modes with respect to the anisotropy ratio $\varepsilon_z'/\varepsilon_x'$. Depending on the combination of the signs of ε_x' and ε_z', the conditions are separated into $\varepsilon_x'<0<\varepsilon_z'$ and $\varepsilon_z'<0<\varepsilon_x'$.

From Eq. (5), it is possible to predict the order of the three lowest resonance frequencies for a nondispersive hyperbolic sphere. When $\varepsilon_x'<0<\varepsilon_z'$, the order of the resonance frequencies is $\omega_{112}<\omega_{111}<\omega_{211}$ as long as $\varepsilon_z'/|\varepsilon_x'|<1/4$. In the same manner, when $\varepsilon_z'<0<\varepsilon_x'$, the order of the resonance frequencies is $\varepsilon_{211}<\varepsilon_{111}<\varepsilon_{112}$ as long as $|\varepsilon_z'|/\varepsilon_x'>5$.

At this stage, we can estimate whether a particular mode exists and what the order of the resonance frequencies is for a hyperbolic sphere. For instance, if $\varepsilon_z'/|\varepsilon_x'|>1/4$ for $\varepsilon_x'<0<\varepsilon_x'$, mode (1, 1, 2) does not exist, and ω_{111} is the lowest frequency among the three modes. Recall that for a high-n isotropic sphere the resonance frequency for mode (1, 1, 1) is always the lowest, and that a lower-order resonance mode resonates at a lower frequency. This is also the case for ordinary waves in a hyperbolic sphere, where resonance occurs for ordinary waves if $\varepsilon_x'>0$. In contrast, for extraordinary waves in a hyperbolic sphere, a lower resonance mode does not necessarily mean a lower resonance frequency, as we have already discussed.

3. RESULTS AND DISCUSSION

To verify the above analysis, we present numerical simulation results for several hyperbolic spheres. Hyperbolic spheres are placed in free space with the optical axis parallel to the z axis. The hyperbolic spheres are irradiated with linearly polarized time-harmonic plane waves to excite the resonance modes. Details of the modeling are provided in [26].

For simplicity, at first we consider four nondispersive hyperbolic spheres that have small losses. While the first two examples (Figs. 1 and 2) are spheres with $\varepsilon_x'<0<\varepsilon_z'$, the other two examples (Figs. 3 and 4) are spheres with $\varepsilon_z'<0<\varepsilon_x'$. The first example is a hyperbolic sphere with a permittivity $(\varepsilon_x,\varepsilon_z)=(-25+0.5i,5+0.1i)$. Since $\varepsilon_x'<0<\varepsilon_z'$ and $\varepsilon_z'/|\varepsilon_x'|<1/4$, we can estimate based on Table 1 that the resonance frequency for mode (1, 1, 2) is the lowest. Figure 1 shows a plot of the absorption efficiency (Q_{abs}) of the sphere together with magnetic field maps for the respective resonance modes. The absorption efficiency is defined as $Q_{\mathrm{abs}}=\sigma_{\mathrm{abs}}/G$, where σ_{abs} is the absorption cross section of the particle and G is the particle cross section [4]. Strong magnetic resonance [mode (1, 1, 1)] as well as electric resonance [mode (1, 1, 2)] are visible. Note that the normalized resonance frequencies ($\omega r/c$) are around or lower than unity,

Table 1. Conditions of the Anisotropy Ratio for the Three Lowest Orders for Extraordinary Waves

	(1, 1, 1)	(1, 1, 2)	(2, 1, 1)
$\varepsilon_x'<0<\varepsilon_z'$	$\varepsilon_z'/\lvert\varepsilon_x'\rvert<1$ $\omega_{111}=\alpha(2/\varepsilon_z'-1/\lvert\varepsilon_x'\rvert)$	$\varepsilon_z'/\lvert\varepsilon_x'\rvert<1/4$ $\omega_{112}=\alpha(2/\varepsilon_z'-4/\lvert\varepsilon_x'\rvert)$	$\varepsilon_z'/\lvert\varepsilon_x'\rvert<4$ $\omega_{211}=\alpha(5/\varepsilon_z'-1/\lvert\varepsilon_x'\rvert)$
$\varepsilon_z'<0<\varepsilon_x'$	$\lvert\varepsilon_z'\rvert/\varepsilon_x'>2$ $\omega_{111}=\alpha(-2/\lvert\varepsilon_z'\rvert)+1/\varepsilon_x')$	$\lvert\varepsilon_z'\rvert/\varepsilon_x'>1/2$ $\omega_{112}=\alpha(-2/\lvert\varepsilon_z'\rvert)+4/\varepsilon_x')$	$\lvert\varepsilon_z'\rvert/\varepsilon_x'>5$ $\omega_{211}=\alpha(-5/\lvert\varepsilon_z'\rvert)+1/\varepsilon_x')$

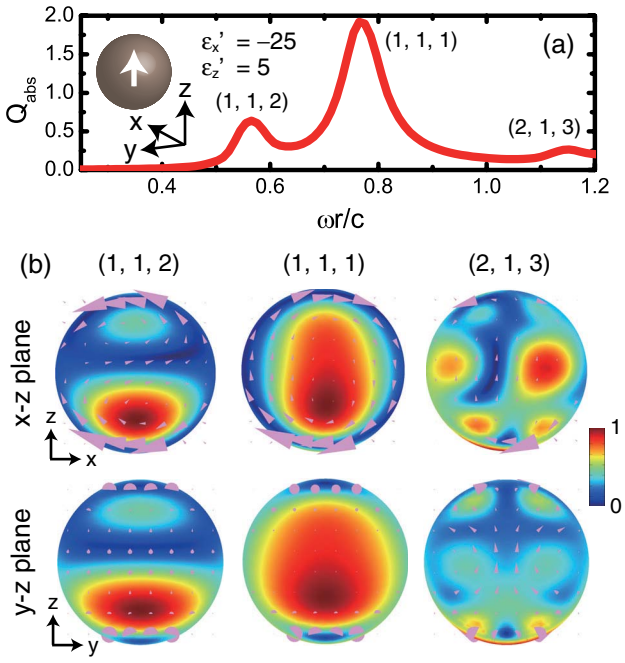

Fig. 1. (a) Absorption efficiency Q_{abs} of a hyperbolic sphere plotted against the normalized frequency where $(\varepsilon_x, \varepsilon_z) = (-25 + 0.5i, 5 + 0.1i)$. Inset shows the coordinates. The white arrow in the sphere in the plot indicates the direction of the optical axis, which is parallel to the z axis. To excite the modes, transverse magnetic polarized $(H \| y)$ plane waves are irradiated at 45° to the x–z plane. (b) Normalized magnetic field amplitudes for the three lowest resonance modes shown in (a). The size of cones is proportional to the magnitude of the electric displacement field.

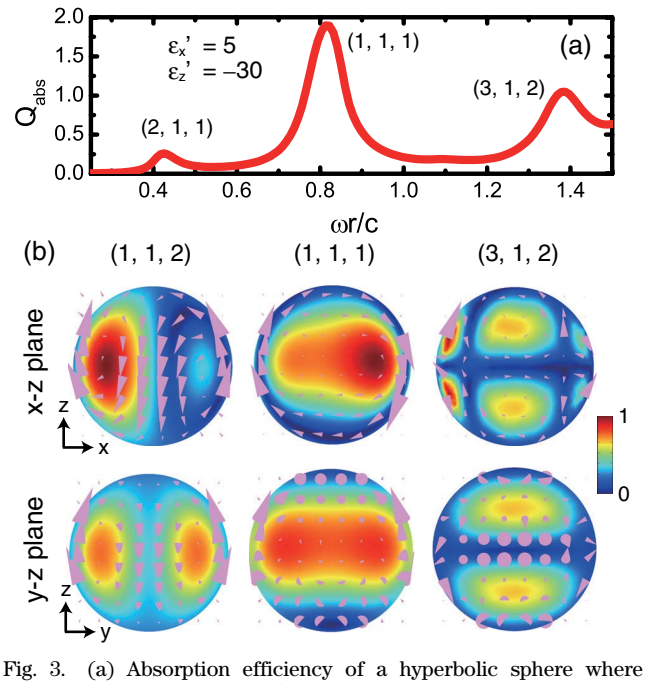

Fig. 3. (a) Absorption efficiency of a hyperbolic sphere where $(\varepsilon_x, \varepsilon_z) = (5 + 0.1i, -30 + 0.6i)$. To excite the modes, transverse magnetic polarized $(H \| y)$ plane waves are irradiated at 45° to the x–z plane. (b) Normalized magnetic field amplitudes for the three lowest resonance modes. The size of cones is proportional to the magnitude of the electric displacement field.

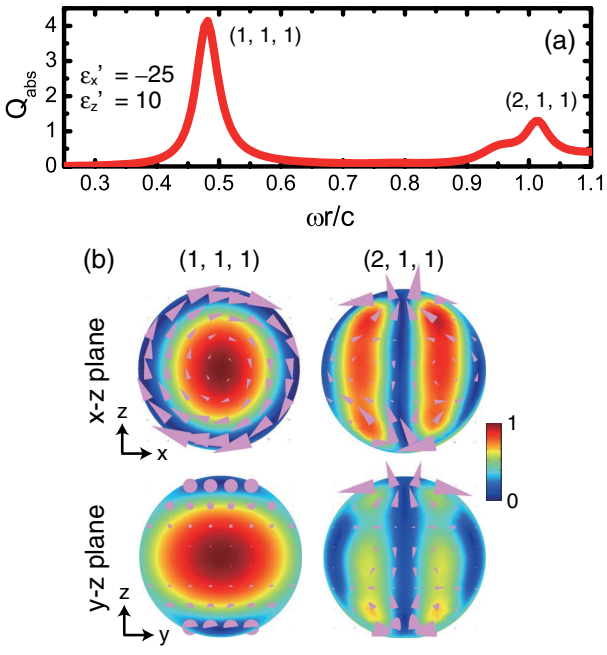

Fig. 2. (a) Absorption efficiency of a hyperbolic sphere where $(\varepsilon_x, \varepsilon_z) = (-25 + 0.5i, 10 + 0.2i)$. To excite these modes, transverse magnetic polarized $(H \| y)$ plane waves are irradiated at 45° to the x–z plane. (b) Normalized magnetic field amplitudes for the two lowest resonance modes. The size of cones is proportional to the magnitude of the electric displacement field.

indicating that hyperbolic spheres act as high-n spheres and resonance occurs for subwavelength spheres. Resonance at low frequencies is also observed in other cases (Figs. 2–5). As expected, mode (1, 1, 2) resonates at the lowest frequency,

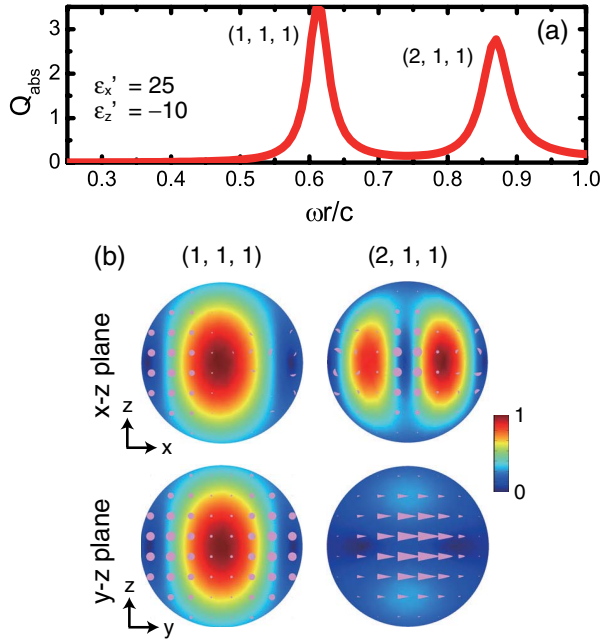

Fig. 4. (a) Absorption efficiency of a hyperbolic sphere where $(\varepsilon_x, \varepsilon_z) = (25 + 0.5i, -10 + 0.2i)$. To excite the modes, transverse electric polarized $(E \| y)$ plane waves are irradiated at 90° to the x–z plane. (b) Normalized magnetic field amplitudes for the two lowest resonance modes. The size of cones is proportional to the magnitude of the electric displacement field. In the x–y plane in mode (1, 1, 1), the electric displacement vectors form a loop (not shown).

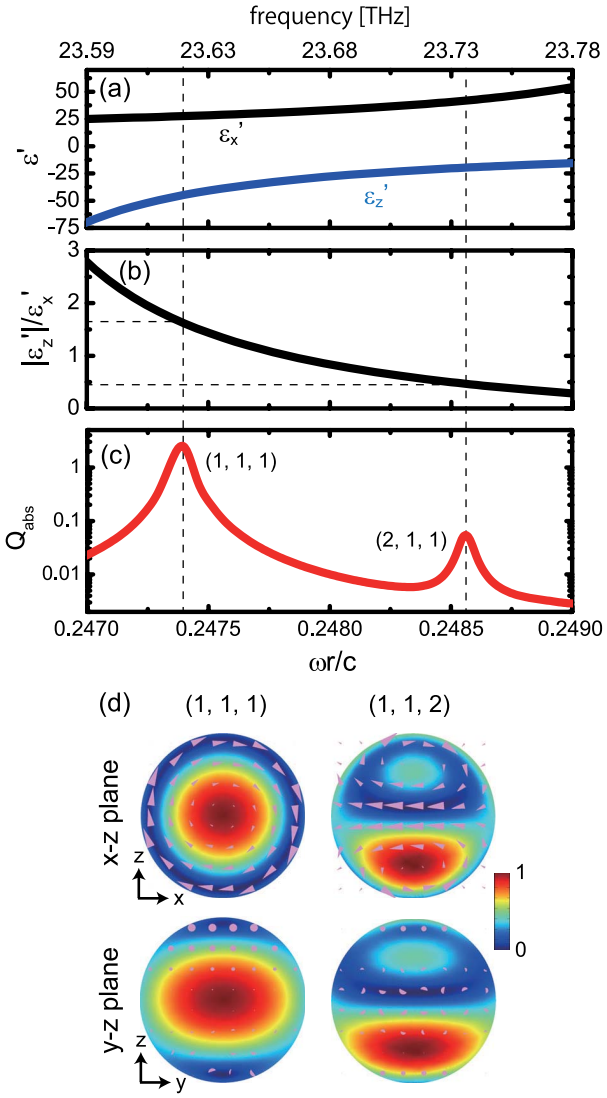

Fig. 5. (a) Permittivity and (b) permittivity ratio of 4H-SiC. (c) Absorption efficiency of a 500 nm 4H-SiC sphere. To excite the modes, transverse magnetic polarized ($H\|y$) plane waves are irradiated at 0° in the x–z plane. (d) Normalized magnetic field amplitudes for the two lowest resonance modes. The size of cones is proportional to the magnitude of the electric displacement field.

and the second-lowest mode is (1, 1, 1). The third mode is not (2, 1, 1) but (2, 1, 3). This is expected because according to Eq. (5) $\omega_{213}(=\alpha(5/\varepsilon'_z - 9/|\varepsilon'_x|)) = 16/25\alpha$ is smaller than $\omega_{112}(=\alpha(2/\varepsilon'_z - 4/|\varepsilon'_x|)) = 24/25\alpha$.

Figure 2 shows results of a hyperbolic sphere where $(\varepsilon_x, \varepsilon_z) = (-25 + 0.5i, 10 + 0.2i)$. Based on Table 1, this sphere should not exhibit mode (1, 1, 2) since $\varepsilon'_z/|\varepsilon'_x| > 1/4$. In Fig. 2(a), mode (1, 1, 2) does not appear, and mode (1, 1, 1) is at the lowest frequency. Subsequently, resonance occurs in mode (2, 1, 1). Since modes (2, 1, 1) and (1, 2, 1) overlap, two antinodes are also seen not only in the x–z plane, but also in the y–z plane [Fig. 2(b)].

Figures 3 and 4 show the resonance modes of hyperbolic spheres where $\varepsilon'_z < 0 < \varepsilon'_x$. Figure 3 shows the simulation results for a hyperbolic sphere with $(\varepsilon_x, \varepsilon_z) = (5 + 0.1i, -30 + 0.6i)$. Since this sphere satisfies the condition $|\varepsilon'_z|/\varepsilon'_x > 4$, resonance occurs in mode (2, 1, 1) before mode (1, 1, 1), as expected based on Table 1. The third mode is (3, 1, 2) because $\omega_{312}(=\alpha(-9/|\varepsilon'_z| + 4/\varepsilon'_x)) = 14/30\alpha$ is smaller than $\omega_{112}(=\alpha(-2/|\varepsilon'_z| + 4/\varepsilon'_x)) = 22/30\alpha$.

Figure 4 shows the simulation results for a hyperbolic sphere with $(\varepsilon_x, \varepsilon_z) = (25 + 0.5i, -10 + 0.2i)$. Since $|\varepsilon'_z|/\varepsilon'_x = 2/5(< 1/2)$, this sphere does not exhibit any of the three modes for extraordinary waves listed in Table 1. However, ordinary waves can contribute to resonance because $\varepsilon'_x > 0$. The resonance modes shown in Fig. 4 are excited by ordinary waves. Considering Eq. (6), we can conclude that resonance occurs in mode (1, 1, 1) at the lowest frequency and subsequently in mode (2, 1, 1), which matches to the results shown in Fig. 4.

Lastly, we consider a dispersive sphere made of 4H-SiC. The permittivity of 4H-SiC is hyperbolic at around 23.6 THz [30]. The radius of the sphere is 500 nm, and the optical axis is aligned to the z axis. Figures 5(a) and 5(b) show a plot of the permittivity of 4H-SiC (taken from [30]) and the anisotropy ratio of 4H-SiC, respectively. Furthermore, Fig. 5(c) shows the absorption efficiency, and the associated modes are shown in Fig. 5(d). The anisotropy ratios in modes (1, 1, 1) and (1, 1, 2) are greater than 1 and 0.25, respectively, both of which satisfy the conditions shown in Table 1. Thus, the guidelines summarized in Table 1 are useful for predicting the resonance modes, even for actual spheres.

4. SUMMARY

In conclusion, we show that hyperbolic spheres can exhibit both magnetic and electric resonances. Due to the effectively high refractive index of hyperbolic materials, low-order resonance modes appear in subwavelength spheres. We presented the conditions necessary for predicting the emergence of resonances and the order of the resonance frequencies for low-order resonance of hyperbolic spheres, which were verified by numerical simulation. Our analysis is also applicable to cubes and can be easily modified for application to cuboids or ellipsoids. Our analysis serves as a concise guideline for finding particular resonance modes of hyperbolic particles that can be used as subwavelength scatterers and absorbers, and as building blocks for metamaterials.

ACKNOWLEDGMENTS

This work was partially supported by the Ministry of Internal Affairs and Communications in Japan under the Strategic Information and Communications R&D Promotion Programme (SCOPE), and by the Murata Science Foundation.

REFERENCES

1. T. Klar, M. Perner, S. Grosse, G. Von Plessen, W. Spirkl, and J. Feldmann, "Surface-plasmon resonances in single metallic nanoparticles," Phys. Rev. Lett. **80**, 4249–4252 (1998).
2. J. Mock, M. Barbic, D. Smith, D. Schultz, and S. Schultz, "Shape effects in plasmon resonance of individual colloidal silver nanoparticles," J. Chem. Phys. **116**, 6755–6759 (2002).
3. H. Kuwata, H. Tamaru, K. Esumi, and K. Miyano, "Resonant light scattering from metal nanoparticles: practical analysis beyond Rayleigh approximation," Appl. Phys. Lett. **83**, 4625–4627 (2003).
4. C. F. Bohren and D. R. Huffman, *Absorption and Scattering of Light by Small Particles* (Wiley, 1983).
5. S. Linden, C. Enkrich, M. Wegener, J. Zhou, T. Koschny, and C. M. Soukoulis, "Magnetic response of metamaterials at 100 terahertz," Science **306**, 1351–1353 (2004).

6. V. M. Shalaev, W. Cai, U. K. Chettiar, H.-K. Yuan, A. K. Sarychev, V. P. Drachev, and A. V. Kildishev, "Negative index of refraction in optical metamaterials," Opt. Lett. **30**, 3356–3358 (2005).
7. S. Zhang, W. Fan, N. Panoiu, K. Malloy, R. Osgood, and S. Brueck, "Experimental demonstration of near-infrared negative-index metamaterials," Phys. Rev. Lett. **95**, 137404 (2005).
8. L. Peng, L. Ran, H. Chen, H. Zhang, J. A. Kong, and T. M. Grzegorczyk, "Experimental observation of left-handed behavior in an array of standard dielectric resonators," Phys. Rev. Lett. **98**, 157403 (2007).
9. Q. Zhao, L. Kang, B. Du, H. Zhao, Q. Xie, X. Huang, B. Li, J. Zhou, and L. Li, "Experimental demonstration of isotropic negative permeability in a three-dimensional dielectric composite," Phys. Rev. Lett. **101**, 027402 (2008).
10. J. A. Schuller, R. Zia, T. Taubner, and M. L. Brongersma, "Dielectric metamaterials based on electric and magnetic resonances of silicon carbide particles," Phys. Rev. Lett. **99**, 107401 (2007).
11. J. C. Ginn, I. Brener, D. W. Peters, J. R. Wendt, J. O. Stevens, P. F. Hines, L. I. Basilio, L. K. Warne, J. F. Ihlefeld, and P. G. Clem, "Realizing optical magnetism from dielectric metamaterials," Phys. Rev. Lett. **108**, 097402 (2012).
12. A. I. Kuznetsov, A. E. Miroshnichenko, Y. H. Fu, J. Zhang, and B. Luk'yanchuk, "Magnetic light," Sci. Rep. **2**, 492 (2012).
13. L. Lewin, "The electrical constants of a material loaded with spherical particles," J. Inst. Electr. Eng. **94**, 65–68 (1947).
14. M. Kerker, D.-S. Wang, and C. Giles, "Electromagnetic scattering by magnetic spheres," J. Opt. Soc. Am. **73**, 765–767 (1983).
15. J. Geffrin, B. García-Cámara, R. Gómez-Medina, P. Albella, L. Froufe-Pérez, C. Eyraud, A. Litman, R. Vaillon, F. González, M. Nieto-Vesperinas, J. Sáenz, and F. Moreno, "Magnetic and electric coherence in forward-and back-scattered electromagnetic waves by a single dielectric subwavelength sphere," Nat. Commun. **3**, 1171 (2012).
16. S. Person, M. Jain, Z. Lapin, J. J. Sáenz, G. Wicks, and L. Novotny, "Demonstration of zero optical backscattering from single nanoparticles," Nano Lett. **13**, 1806–1809 (2013).
17. V. Y. Davydov, Y. E. Kitaev, I. N. Goncharuk, A. N. Smirnov, J. Graul, O. Semchinova, D. Uffmann, M. B. Smirnov, A. P. Mirgorodsky, and R. A. Evarestov, "Phonon dispersion and Raman scattering in hexagonal GaN and AlN," Phys. Rev. B **58**, 12899 (1998).
18. R. Gómez-Medina, B. García-Cámara, I. Suárez-Lacalle, F. González, F. Moreno, M. Nieto-Vesperinas, and J. J. Sáenz, "Electric and magnetic dipolar response of germanium nanospheres: interference effects, scattering anisotropy, and optical forces," J. Nanophotonics **5**, 053512 (2011).
19. L. Qin, D.-X. Qi, F. Gao, R.-W. Peng, J. Zou, Q.-J. Wang, and M. Wang, "Tunable electric and magnetic resonances in multilayered metal/dielectric nanoplates at optical frequencies," J. Phys. D **43**, 345102 (2010).
20. L. V. Alekseyev, V. A. Podolskiy, and E. E. Narimanov, "Homogeneous hyperbolic systems for terahertz and far-infrared frequencies," Adv. Optoelectron. **2012**, 267564 (2012).
21. Z. Liu, H. Lee, Y. Xiong, C. Sun, and X. Zhang, "Far-field optical hyperlens magnifying sub-diffraction-limited objects," Science **315**, 1686 (2007).
22. A. J. Hoffman, L. Alekseyev, S. S. Howard, K. J. Franz, D. Wasserman, V. A. Podolskiy, E. E. Narimanov, D. L. Sivco, and C. Gmachl, "Negative refraction in semiconductor metamaterials," Nat. Mater. **6**, 946–950 (2007).
23. J. Yao, Z. Liu, Y. Liu, Y. Wang, C. Sun, G. Bartal, A. M. Stacy, and X. Zhang, "Optical negative refraction in bulk metamaterials of nanowires," Science **321**, 930 (2008).
24. J. Yao, X. Yang, X. Yin, G. Bartal, and X. Zhang, "Three-dimensional nanometer-scale optical cavities of indefinite medium," Proc. Natl. Acad. Sci. USA **108**, 11327–11331 (2011).
25. X. Yang, J. Yao, J. Rho, X. Yin, and X. Zhang, "Experimental realization of three-dimensional indefinite cavities at the nanoscale with anomalous scaling laws," Nat. Photonics **6**, 450–454 (2012).
26. S. Ishii, S.-i. Inoue, and A. Otomo, "Scattering and absorption from strongly anisotropic nanoparticles," Opt. Express **21**, 23181–23187 (2013).
27. D. Li, L. Qin, X. Xiong, R.-W. Peng, Q. Hu, G.-B. Ma, H.-S. Zhou, and M. Wang, "Exchange of electric and magnetic resonances in multilayered metal/dielectric nanoplates," Opt. Express **19**, 22942–22949 (2011).
28. W. T. Chen, M. L. Tseng, C. Y. Liao, P. C. Wu, S. Sun, Y.-W. Huang, C. M. Chang, C. H. Lu, L. Zhou, and D.-W. Huang, "Fabrication of three-dimensional plasmonic cavity by femtosecond laser-induced forward transfer," Opt. Express **21**, 618–625 (2013).
29. A. Yariv and P. Yeh, *Optical Waves in Crystals* (Wiley, 1984).
30. H. Mutschke, A. C. Andersen, D. Clement, T. Henning, and G. Peiter, "Infrared properties of SiC particles," Astron. Astrophys. **345**, 187–202 (1999).